

Prominent Region of Interest Contrast Enhancement for Knee MR Images: Data from the OAI

Joyce Sia Sin Yin*, Tan Tian Swee, Azli Bin Yahya, Matthias Tiong Foh Thye, Kelvin Ling Chia Hiik, Leong Kah Meng,
Tan Jia Hou & Sameen Ahmed Malik

^aBiomedical Engineering Programme,
School of Biomedical Engineering and Health Sciences,
Faculty of Engineering, Universiti Teknologi Malaysia, Malaysia

Hum Yan Chai

^bDepartment of Mechatronics and Biomedical Engineering,
Lee Kong Chian Faculty of Engineering and Science,
Universiti Tunku Abdul Rahman, Malaysia

Khairil Amir Bin Sayuti & Ahmad Tarmizi Musa

^cDepartment of Radiology,
Universiti Sains Malaysia, Malaysia

*Corresponding author: tantswee@biomedical.utm.my

Received 12 August 2019, Received in revised form 16 February 2020
Accepted 30 March 2020, Available online 30 August 2020

ABSTRACT

Osteoarthritis is the most commonly seen arthritis, where there are 30.8 million adults affected in 2015. Magnetic resonance imaging (MRI) plays a key role to provide direct visualization and quantitative measurement on knee cartilage to monitor the osteoarthritis progression. However, the visual quality of MRI data can be influenced by poor background luminance, complex human knee anatomy, and indistinctive tissue contrast. Typical histogram equalisation methods are proven to be irrelevant in processing the biomedical images due to their steep cumulative density function (CDF) mapping curve which could result in severe washout and distortion on subject details. In this paper, the prominent region of interest contrast enhancement method (PROICE) is proposed to separate the original histogram of a 16-bit biomedical image into two Gaussians that cover dark pixels region and bright pixels region respectively. After obtaining the mean of the brighter region, where our ROI – knee cartilage falls, the mean becomes a break point to process two Bezier transform curves separately. The Bezier curves are then combined to replace the typical CDF curve to equalize the original histogram. The enhanced image preserves knee feature as well as region of interest (ROI) mean brightness. The image enhancement performance tests show that PROICE has achieved the highest peak signal-to-noise ratio (PSNR=24.747±1.315dB), lowest absolute mean brightness error (AMBE=0.020±0.007) and notably structural similarity index (SSIM=0.935±0.019). In other words, PROICE has considerably outperformed the other approaches in terms of its noise reduction, perceived image quality, its precision and has shown great potential to visually assist physicians in their diagnosis and decision-making process.

Keywords: Osteoarthritis; magnetic resonance imaging; contrast enhancement; mean of the brighter region; knee cartilage

INTRODUCTION

From the data analysis of year 2013 to 2015 from National Health Interview Survey, 54.4 million (one in five adults) adults in the United States are having doctor-diagnosed arthritis (Barbour et al. 2017). However, osteoarthritis (OA) is the most common seen arthritis where 30.8 million adults are affected in 2015 (Cisternas et al. 2016). To monitor the OA progression, magnetic resonance (MR) imaging play a key role to give direct visualization and quantitative measurement on knee cartilage. However, MRI data are prone to imaging artifacts and easily affected by acquisition noise (Styner et al. 2000).

Visual quality of human knee MR images can be influenced by poor background luminance, complex human knee structure and indistinctive tissue contrast. In clinical routine, excellent MRI soft-tissue contrast could facilitate the image interpretation process. Unfortunately, mediocre knee images with poor low contrast were obtained in normal circumstances. For instances, the contrast of fat, surrounding cartilage tissue, cartilage and fluid are not distinctive which might lead to ambiguity of both inter- and intra-observer during delineation process. Human knee has complex anatomical structure which cause the delineation on poor-contrast knee MR images to be laborious and time consuming (Gan, Swee, et al. 2014; Dougherty 2009).

Besides, MR images may be corrupted by unwanted artifacts and noise (Dar et al. 2019). Therefore, pre-processing step comes into the first place to remove noise, to sharpen details or edges and also to enhance the image contrast. Knee MR images consists big portions of low intensity pixels which represent the backgrounds, tibial and femoral bones. Hence, conventional contrast enhancement with histogram equalization (HE) is unsuitable for medical image processing. Conventional HE naively diverges the dynamic range coverage of the object image which results distortion of image brightness. The resultant image might lose any brightness sensitive image feature. Moreover, traditional HE tends to combine the light probability density gray level with higher probability density gray level to widen the gap in between. This results a sudden jump while calculating its cumulative density function that could over-enhance the image (Gan, Swee, et al. 2014).

In this paper, a new contrast enhancement framework known as prominent region of interest contrast enhancement (PROICE), which extended from BBCCE (Gan, Swee, et al. 2014), is proposed. From the input histogram, the 16-bit DICOM image will be characterized into two intensity groups, one group of low intensity pixels and another group of high intensity pixels. The mean of the higher intensity pixels is obtained to preserve the mean brightness of the region of interest (ROI), human knee cartilage. The histogram equalization remapping process is performed based on Bezier curve transformation, replacing the conventional cumulative density function to improve the visual perception of ROI and conserve the knee features for further image processing stages. Single right knee MR scan is selected from 100 different subjects to ensure wide variability of knee structure and image contrast to be studied. We examine PROICE with several performance metrics in terms of peak signal -to-noise ratio (PSNR), absolute mean brightness error (AMBE), structural similarity index (SSIM), number of detected edges (#DE) and computation time.

RELATED WORKS

BACKGROUND OF HISTOGRAM EQUALIZATION

HE is a popular method for image contrast enhancement. From a normalized histogram, every occurrence probability of a pixel of certain intensity is calculated known as probability density function (PDF), $p(x)$. Later, all the probabilities are summed up to obtain cumulative distribution function (CDF) which becomes the transform function to map the original input histogram for a better appearance. However, the global transform which prone to merge lower possibilities gray levels with other higher possibilities gray levels occurrence could deteriorate the resultant image quality (Dougherty 2009).

Over the past twenty years, researchers have been actively finding better contrast enhancement frameworks, for instances high frequency gray level removal, histogram separation, other advanced method and some with the

involvement of artificial intelligence. These will be discussed further in the rest of this section.

CLIPPING AND ELIMINATION OF CERTAIN HIGH FREQUENCY INTENSITY LEVELS

In 1990, Stephen proposed a local contrast enhancement method, named contrast-limited adaptive HE (CLAHE) which modified the ordinary HE by capping the maximum intensity level. CLAHE implemented interactive intensity windowing which allows detection of small intensity changes referring to neighbouring pixels, thus able to reduce the noise in relatively homogeneous areas (Pizer et al. 1990). On the other hand, multipeak HE was introduced by Wongsritong to equalize every detected peak in the input histogram (Wongsritong et al. 1998). Instead of processing two sub-histograms, Majid Zarie introduced triple dynamic HE (TDCHE) which partitioned the histogram into three sub-histograms. Clipping process was performed in each sub-histogram based on their respective mean or median then the partitions were remapped into a new dynamic range before equalization process was performed (Zarie, Hajghassem, and Majd 2018). With the capping and redistributing intensity features, methods aforementioned manage to improve the image local contrast and boundary features. Furthermore, gamma correction adaptive extreme-level eliminating with weighting distribution (GCAELEWD) to eliminate the PDF of two extreme levels on each divided sub-block and reconstruct the image using bilinear interpolation technique was reported. The author claimed that the removal of extremes could increase the difference of intensities on medical images (Teh, Sim, and Wong 2018).

HISTOGRAM SEPARATION

In 1997, Kim made a major breakthrough claiming that preserving the mean brightness of the image is necessary for natural enhancement. He then introduced mean-preserving bi-histogram equalization (BBHE) that divides input image into two sub-images based on its mean and equalizes them respectively (Kim 1997). Inspired by BBHE, Yu Wang et al. proposed equal area dualistic sub-image HE (DSIHE) which decomposes the input histogram into two equal-size histograms based on its median. The author claimed that DSIHE can prevent the original image average brightness from huge deviation (Wang, Chen, and Zhang 1999). Later, researchers started to hypothesize that a better contrast enhancement could be expected if histogram could be separated numerously. Soon, Soong-Der Chen et al. convinced that recursive mean-separate HE (RMSHE) could result in better enhancement results than BBHE by separating the decomposed histograms recursively with their new means (Chen and Ramli 2003a). However, RMSHE is computation heavy and time-consuming at that point. In the same year, the author introduced minimum mean brightness bi-HE (MMBEBHE) which separated histogram pre-determined threshold level that results from the lowest absolute mean brightness error (AMBE) (Chen and Ramli

2003b). In conventional HE, gray levels with higher frequencies tend to dominate other gray levels of lower frequencies. To overcome the problem, M. Abdullah et al. and Wan Zakiah Wan Ismail proposed dynamic HE (DHE) to partition the histograms into several sub-histograms and each only allowed to occupy certain gray level so as to preserve the appearance of lower frequencies pixels (Abdullah-Al-Wadud et al. 2007; Ismail and Sim 2011). Shih-Chia Huang et al. suggested a new histogram separation framework based on multiple thresholding procedures and the most favourable peak signal-to-noise ratio (PSNR) (Huang and Yeh 2013). Meanwhile, Sabyasachi et al. revealed hyper kurtosis based modified duo-histogram equalization (HKMDE) and tested on human brain CT scan images. It separates histogram into two based on the modified mean (MM) (Mukhopadhyay et al. 2015).

For years, researchers have been lingering in histogram separation to improve the enhancement effect but there is no significant changes being observed until today. In 2013, Fan-Chieh Cheng et al. pointed out that Bezier curve could be an ideal alternative to replace the typical CDF curve for mapping process. All the control points and mapping curves are done through automatic calculation (Cheng and Huang 2013). The author claimed that Bezier curve could overcome the washed-out effect due to its gentle curve which diverges intensity distribution gradually. Gan et al. was then inspired to implement spline curve in enhancing knee MR images partitioned based on its median (Gan, Tan, et al. 2014). Later, Gan et al. highlighted bi-histogram Bezier curve contrast enhancement (BBCCE) in processing the medical images that have indistinctive tissue contrasts and poor background luminance. BBCCE replaces the conventional cumulative density function with its own generated Bezier transform curve (Gan, Swee, et al. 2014). Meanwhile, Asghar et al. also introduced the separation of high frequency gray levels with high pass filter while low frequency gray levels with low pass filter, and equalize them respectively with Bezier curve in order to preserve the small details (Asghar et al. 2017).

OTHER ADVANCED FRAMEWORK

Sampada et al. suggested to combine both local and global method which preserved the details and overall brightness of the image (Pathak, Dahiwal, and Padole 2015). On the other hand, the variational-based model uncovered by Tian et al. resulted an enhanced image that shows the trade-off between global and local contrast enhancement (Tian and Cohen 2018). Most HE might cause the disappearance of small size objects. Therefore, Elena et al. proposed to have parameters estimation of the details which focused on object boundaries to generate several contrast kernels defined with weighted contrast and relative contrast (Yelmanova and Romanyshyn 2017b, 2017a, 2017c), herewith, another approach that referred the relative strength between targeted pixels with adjacent pixels (Wang, Huang, and Hu 2018).

There is a finding that high quality images can be produced by fusing pseudo multi-exposure images which could be generated from the original image (Kinoshita and Kiya 2018). For hazy image processing, partial differential equation-based contrast enhancement locally and globally is reported. Optimization of gradient based metrics are referred as stopping criteria (Nnolim 2018). According to Yang et al., choosing two suitable Gamma curves to deal with both dark and bright regions of the image is beneficial for both high dynamic range (HDR) and low dynamic range (LDR) compression (Yang et al. 2018). Another work from Singh et al. on swarm intelligence optimized piecewise gamma corrected HE to solve over-saturation and unnatural artifacts that could normally be occur on dark satellite images and biomedical images (Singh et al. 2018).

In recent years, as AI starts booming in all fields of industries, and likewise, the researchers working with image processing started to find its potential in contributing better algorithms. Anita et al. introduced fuzzy contrast mapping to map the gray level to suitable membership function (Thakur and Mishra 2015). The method enhances gray levels which are closer to mean gray level and produce result image with a more decent contrast than its original image (Mamoria and Raj 2016). Meanwhile, Shweta et al. proposed artificial neural network (ANN) and fuzzy logic in image enhancement. ANN is used to identify the type of noises while fuzzy logic is used for denoising and contrast enhancement (Narnaware and Khedgaonkar 2015). Arushi et al. and Leonardo et al. suggested to combine the Gaussian mixture model and genetic algorithm for input histogram partition and contrast enhancement (Mahajan and Gupta 2017; Rundo et al. 2019).

METHODOLOGY

MR IMAGE ACQUISITION

One hundred dual-echo steady-state (DESS) knee MR images with water excitation (we) were obtained from the 18-month visit package provided by Osteoarthritis Initiative (OAI). MR machine that used to acquire these images is Siemens Magnetom Trio from Germany. The acquired MR images have section thickness of 0.7mm and in-plane resolution of 0.365 x 0.456mm. Other technical parameters upon acquisition are stated as: field of view = 140 x 140 mm, flip angle of 25°, TR/TE = 16.3/4.7m sec, bandwidth = 185Hz/pixel and matrix size of 384 x 384 mm. Further information can be obtained from the following website: <https://nda.nih.gov/oai>

SOFTWARE AND COMPUTER SPECIFICATIONS

All the algorithms and performance tests mentioned are run through MATLAB 2019a on a laptop hosting Intel Core i7-6700HQ quad core with hyper-threading clocked at 2.6 – 3.5GHz, 8GB DDR4 RAM and NVIDIA GTX960M (4GB GDDR5 RAM).

GAUSSIAN MIXTURE MODEL

A Gaussian mixture is a function which comprises of several Gaussians. The observations x , from mixture model with K mixture components, the marginal probability distribution of x is written in the Equation (1):

$$P(x) = \sum_{j=1}^K w_j \cdot N(x; \mu_j, \sigma_j^2) \quad (1)$$

where $j \in \{1, 2, \dots, K\}$ is the latent variable representing the mixtures component for X_i . Meanwhile, $N(x; \mu_j, \sigma_j^2)$ represents the Gaussian mixtures and w_j is the mixture proportion to identify which -th cluster does the X_i belong to.

Given a set of data $X = \{x_1, x_2, \dots, x_N\}$, the parameter θ of the GMM model can be estimated to fit the data as follows in Equation (2):

$$\begin{aligned} \theta^* &= \operatorname{argmax}_{\theta} p(X|\theta) \\ \theta^* &= \operatorname{argmax}_{\theta} \prod_{i=1}^N p(x_i | \theta) \end{aligned} \quad (2)$$

The most widely used approach to maximize the likelihood $p(x_i|\theta)$ of the data based on the model parameters is Expectation-Maximization (EM) algorithm. E-step is to estimate the probability of the points generated by each Gaussian. Meanwhile, M-step is a maximization to improve the likelihood of the data according to a hidden variable, Z . Likelihood, L can be written as follows in Equation (3):

$$\begin{aligned} L(X, Z, \theta) &= p(X, Z | \theta) \\ &= \prod_{i=1}^N \prod_{j=1}^K [p(x_i, j | \theta)]^{z_{ij}} \\ &= \prod_{i=1}^N \prod_{j=1}^K [p(x_i | j, \theta)]^{z_{ij}} [p(j | \theta)]^{z_{ij}} \end{aligned} \quad (3)$$

The equation (3) can be further expressed in logarithm form as shown in Equation (4).

$$\log[p(X, Z)] = \sum_{i=1}^N \sum_{j=1}^K z_{ij} \log[p(x_i | j, \theta)] + z_{ij} \log[p(j | \theta)] \quad (4)$$

Referring Figure 1 (a) and (b), the knee MR image has poor background luminance, indistinctive tissue contrast, and most of the pixels fall onto gray levels that skewed to the left. However, our interest is the human knee cartilage which falls onto the higher gray levels and it occupies the minority of the pixels. To avoid the wash out effect on our

ROI, the mean brightness of cartilage must be conserved. Therefore, GMM comes in place to cluster the original histogram into two Gaussians, first Gaussian on darker region while second Gaussian on brighter region. Later, mean brightness of the second Gaussian is obtained to decompose the original histogram into two sub-histograms for further pre-processing stage.

OBTAINING INTENSITY DISCREPANCY VALUE

In Figure 1(e), a sudden leap in CDF curve could result severe intensity distortion. However, the curve can be further smoothed by lowering down the absolute intensity difference (AID), which can be illustrated as follows in Equation (5):

$$AID = x' - x \quad (5)$$

where x represents original intensity distribution while x' represents the transformed intensity distribution. The higher the AID, the higher the degree of enhancement and prone to wash out the details of the cartilage. Deduction between CDF curve and linear curve results an intensity discrepancy to identify the critical points that later would be the vital components to generate Bezier transform curve.

Given that intensity discrepancy value, $IDV \in \mathbb{R}$, assist to determine the points with its gradient, $\frac{dy}{dx} = 0$. Local minimum and local maximum points can be determined with $\frac{d^2y}{dx^2} > 0$ and $\frac{d^2y}{dx^2} < 0$ respectively. Boundary condition of $y = 0$ is subjected to all the critical points and therefore minimum point will fall in region $y < 0$ while maximum point will lie in region $y > 0$. Meanwhile, global maximum and global minimum can be obtained by taking the extrema value in each region as shown in Equation (6) and Equation (7) respectively.

$$P_{Global\ maximum}(x) \begin{cases} \operatorname{Argmax}(IDV); & y > 0 \\ 0 & ; \text{otherwise.} \end{cases} \quad (6)$$

$$P_{Global\ minimum}(x) \begin{cases} \operatorname{Argmin}(IDV); & y < 0 \\ 0 & ; \text{otherwise.} \end{cases} \quad (7)$$

As the histogram is decomposed into two sub-histograms by GMM, the IDVs are calculated respectively which results a total of two pairs of critical points.

BEZIER CURVE TRANSFORMATION

Bezier curve is a parametric convex curve, delineates its shape by the end points and the control points given. The curve is formed within a control polygon which avoid itself from derailing off the polygon. Bezier curve has a smoother shape compared to typical CDF curve, thus smaller AID can

be expected. Let the control points denoted as $C_0, C_1, C_2, \dots, C_n$, bounded within the domain $t \in [0,1]$ where the control points are the critical points, P obtained in the previous stage. Bezier curve is defined as follows in Equation (8):

$$Q(t) = \sum_{i=0}^n B_{n,i}(t) C_i \quad (8)$$

Bezier curve utilizes Bernstein polynomials as a basis and can be illustrated as shown in Equation (9).

$$B_{n,i}(t) = \binom{n}{i} t^i (1-t)^{n-i} \quad (9)$$

The binomial coefficient is shown in Equation (10).

$$\binom{n}{i} = \begin{cases} \frac{n!}{i!(n-i)!}, & \text{if } 0 \leq i \leq n \\ 0, & \text{otherwise} \end{cases} \quad (10)$$

In this paper, the Bezier curve of second or third degree is more likely to be formed based on the number of global extrema detected. There are four control points if a pair of global extrema is detected and therefore, a third degree Bezier curve will be formed. Meanwhile, if there are only ($n = 3$) three control points, a second degree ($n = 2$) Bezier curve will be generated.

ASSESSMENT METHODOLOGY

Notably, the image processed is 16-bit, compared to 8-bit gray image test on other previous work. The details of the image are conserved to its optimum with its full dynamic range. For a fair test, all the other methods (HE, BBHE, DSIHE and BBCCE) are tested with the same group of 16-bit images. Then, the performance of each resultant images is evaluated from several statistical analysis in terms of peak signal-to-noise ratio (PSNR), absolute mean brightness error (AMBE), structural similarity (SSIM), number of detected edges (#DE) and computation time.

Let I_{ori} and I_{en} be the original input image and the enhanced image respectively. The gray levels of input image, $L_{in} = l_{in}^{min}, \dots, l_{in}^{max}$ and $L_{out} = l_{out}^{min}, \dots, l_{out}^{max}$ for the output image. The PSNR indicates the ratio between the maximum possible intensity value of the input image and the average squares of the errors between the input and output images as shown in Equation (11):

$$\begin{aligned} PSNR &= 10 \log_{10} \left(\frac{l_{in}^{max2}}{MSE} \right) \\ &= 20 \log_{10} \left(\frac{l_{in}^{max2}}{\sqrt{MSE}} \right) \end{aligned} \quad (11)$$

Considering the image consists of M rows and N columns. Mean squared error, MSE can determine the deviation of output image from its original input image which can be denoted as shown in Equation (12):

$$\begin{aligned} \text{MSE} \\ &= \frac{1}{M \times N} \sum_{a=1}^M \sum_{b=1}^N I_{ori}(a,b) - I_{en}(a,b)^2 \end{aligned} \quad (12)$$

MSE is always positive and denotes a better result when its value is closer to zero. AMBE can measure the overall brightness preservation of the resultant image:

$$AMBE = \frac{|Mean_{I_{ori}} - Mean_{I_{en}}|}{L} \quad (13)$$

where L is the dynamic range of the input image as shown in Equation (14);

$$L = l_{in}^{max} - l_{in}^{min} \quad (14)$$

SSIM index is a predictive method to measure the similarity between enhanced image and original image. Structural information is the strong dependencies of the pixels that represent the structure of objects in an image. SSIM is measuring the degradation of structural information of the structures in the image. SSIM formula consists of three comparison measurements which are luminance (l), contrast (c) and structure (s), let $I_{ori} = x, I_{en} = y$ are shown in Equation (15), Equation (16) and Equation (17) respectively.

$$\text{Luminance comparison, } l(x,y) = \frac{2\mu_x\mu_y + k_1}{\mu_x^2 + \mu_y^2 + k_1} \quad (15)$$

$$\text{Contrast comparison, } c(x,y) = \frac{2\sigma_x\sigma_y + k_2}{\sigma_x^2 + \sigma_y^2 + k_2} \quad (16)$$

$$\text{Structural comparison, } s(x,y) = \frac{\sigma_{xy} + k_3}{\sigma_x\sigma_y + k_3} \quad (17)$$

where $\mu_x, \mu_y, \sigma_x, \sigma_y$ and σ_{xy} are the local means, standard deviations and the cross-variance for the original image and enhanced image respectively. Meanwhile, $k_1, k_2, k_3 \in \mathbb{R}^+$ are regularization constants for the three comparisons. The three comparisons are combined as shown in Equation (18):

$$SSIM = l(x,y)^\alpha \cdot c(x,y)^\beta \cdot s(x,y)^\gamma \quad (18)$$

where α, β and γ are the weighting components and equal to one. Then, SSIM can be written as shown in Equation (19):

$$SSIM = \frac{(2\mu_x\mu_y + k_1)(2\sigma_{xy} + k_2)}{(\mu_x^2 + \mu_y^2 + k_1)(\sigma_x^2 + \sigma_y^2 + k_2)} \quad (19)$$

High SSIM value indicates that the enhanced image and the original image are quantitatively similar.

Number of edges detected could determine the effectiveness of the contrast enhancement method. More edges shall be observed in enhanced images, compared to its original image. Canny, is a highly reliable edge detector. By applying double thresholding and hysteresis-based edge tracking, it can identify the less-visible edges.

Let M_{canny} be the edge map, number of edges detected is as shown in Equation (20):

$$\#DE = \sum_{a=1}^M \sum_{b=1}^N M_{canny}(a,b) \quad (20)$$

Figure 1 shows the PROICE framework in enhancing knee MR images.

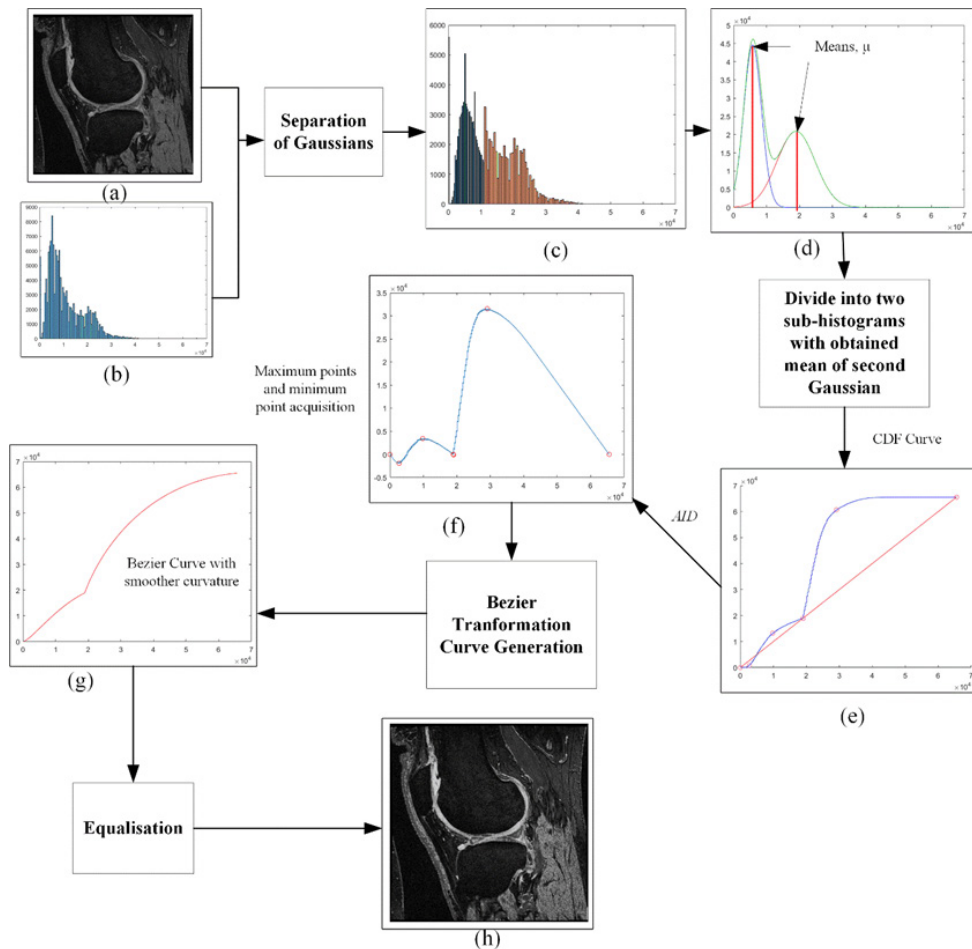


FIGURE 1. PROICE framework in enhancing knee MR images. (a) Original sagittal knee MR image. (b) Original histogram. (c) Clustered Gaussians with GMM. (d) Clustered Gaussian curves for high gray level group and low gray level group. (e) Blue line indicated typical CDF curve. (f) Intensity discrepancy curve generated from CDF curve. (g) Bezier transform curve as replacement of CDF curve. (h) Enhanced image with proposed method

STATISTICAL ANALYSIS

Figure 2 shows the Boxplots of the image enhancement performance evaluation metrics obtained from 16-bit 100 MR knee images enhanced with HE, BBHE, DSIHE, BBCCE and proposed method. The lower and upper boundary of each boxplot indicates the first (25th percentile) and third quartiles (75th percentile) of the distribution, interquartile range can be identified by obtaining differences in these quartiles.

Mean and median are represented by a black cross and a black line respectively. Outliers are displayed as coloured small dots.

Table 1 shows median, mean and standard deviation of image enhancement performance evaluation metrics (PSNR, AMBE and SSIM) tested with HE, BBHE, DSIHE, BBCCE and PROICE on a total of 100 knee MR images. Table 2 shows median, mean and standard deviation of image enhancement performance evaluation metrics (#DE and Time Consumption) tested with HE, BBHE, DSIHE, BBCCE and PROICE on a total of 100 knee MR images.

Most of the state-of-art enhancement methods aim to enhance the contrast of whole image. However, human knee has the most complex bone anatomy hence the cartilage segmentation can be very time consuming due to poor luminance and contrast differences between the hyaline cartilage with neighbouring tissues. Therefore, PROICE is proposed focusing on only our ROI, which falls on higher gray levels. From Figure 3 And Table 1, PROICE achieves the highest PSNR value (24.747 ± 1.315 dB) and followed by

BBCCE method (20.041 ± 0.755 dB). The standard deviation resulted by PROICE is slightly higher that generates more variability of enhancement performance compared to other methods. The proposed method tends to enhance the brighter regions in the MR image, which cover our ROI. Therefore, PROICE spreads the bright intensity pixels referring to their original distribution. It tends to stretch the bright pixels to cover wider dynamic range which results in a more distinctive contrast difference between fat, cartilages,

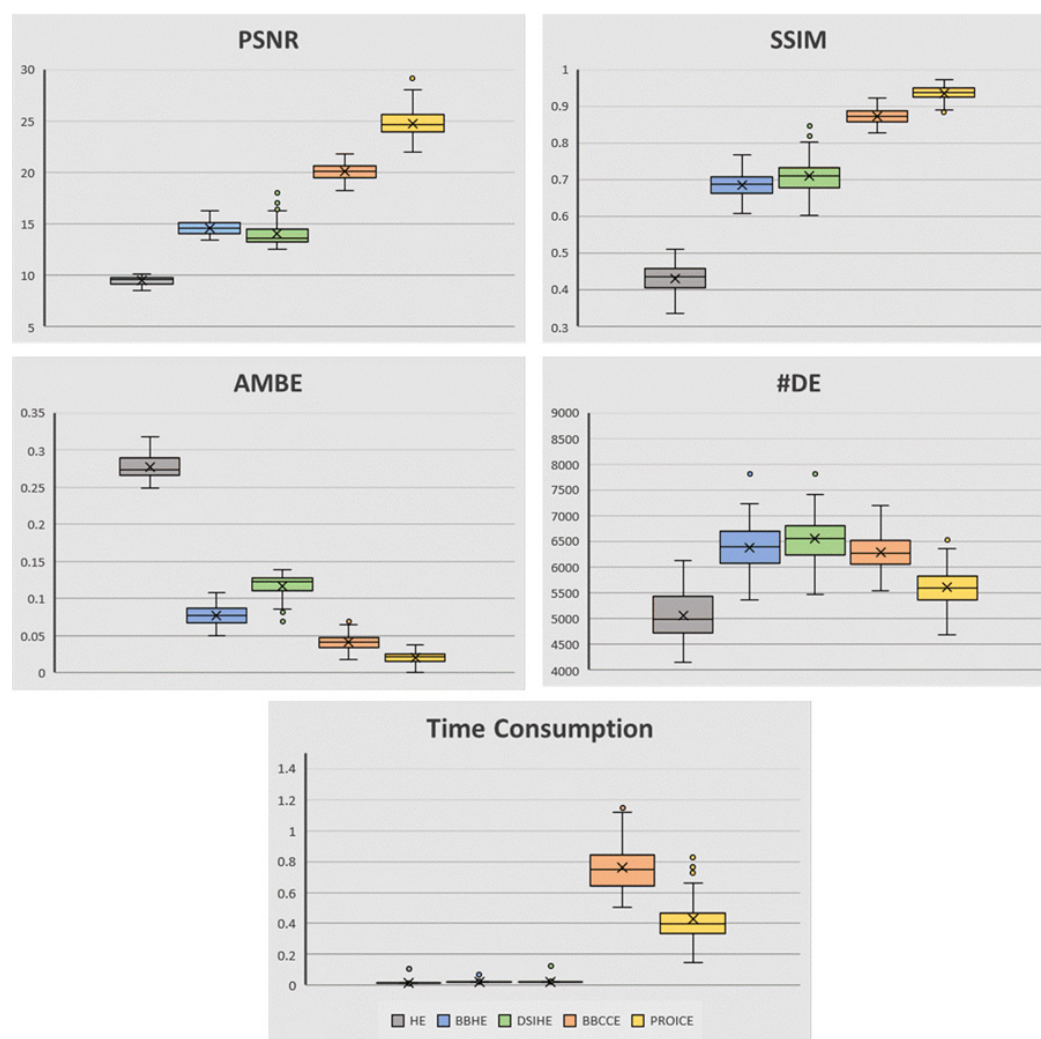


FIGURE 2. Boxplots of the image enhancement performance evaluation metrics obtained from 16-bit 100 MR knee images enhanced with HE, BBHE, DSIHE, BBCCE and proposed method

TABLE 1. Median, mean and standard deviation of image enhancement performance evaluation metrics (PSNR, AMBE and SSIM) tested with HE, BBHE, DSIHE, BBCCE and PROICE on a total of 100 knee MR images

	PSNR			AMBE			SSIM		
	Median	Mean	Std. Dev.	Median	Mean	Std. Dev.	Median	Mean	Std. Dev.
HE	9.471	9.471	0.386	0.273	0.277	0.016	0.436	0.430	0.037
BBHE	14.536	14.588	0.709	0.077	0.077	0.013	0.686	0.685	0.031
DSIHE	13.584	14.010	1.252	0.122	0.117	0.015	0.711	0.710	0.048
BBCCE	20.067	20.041	0.755	0.041	0.041	0.010	0.873	0.873	0.020
PROICE	24.607	24.747	1.315	0.021	0.020	0.007	0.936	0.935	0.019

TABLE 2. Median, mean and standard deviation of image enhancement performance evaluation metrics (#DE and Time Consumption) tested with HE, BBHE, DSIHE, BBCCE and PROICE on a total of 100 knee MR images

	#DE			Time		
	Median	Mean	Std. Dev.	Median	Mean	Std. Dev.
HE	4990.500	5063.160	459.762	0.013	0.014	0.010
BBHE	6398.000	6373.040	456.118	0.020	0.021	0.005
DSIHE	6552.000	6557.090	422.112	0.019	0.020	0.011
BBCCE	6264.500	6293.510	338.673	0.748	0.758	0.187
PROICE	5585.500	5600.600	367.724	0.399	0.425	0.215

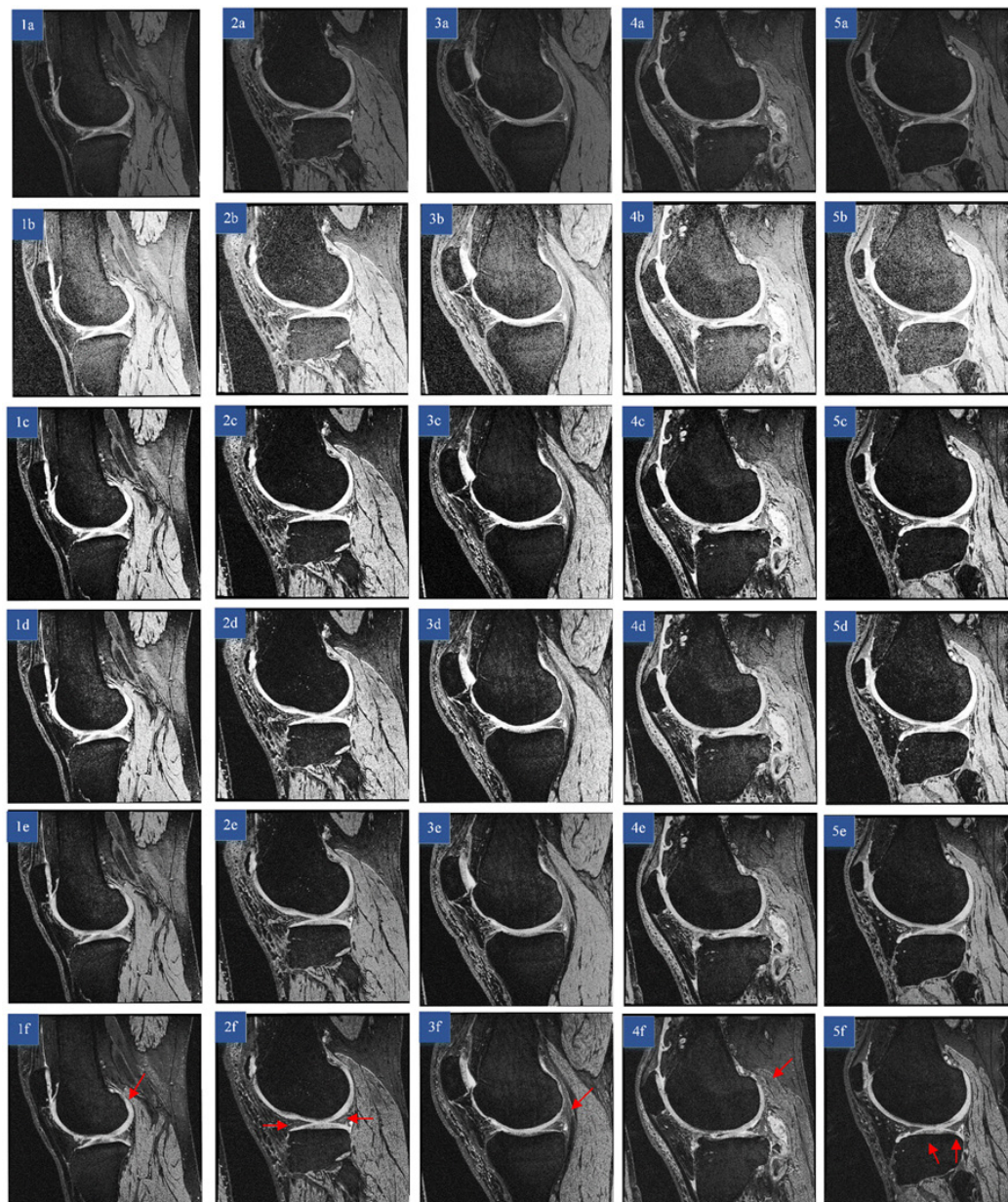


FIGURE 3. Visual result evaluation and methods comparisons. (1a-5a) Five original knee MR images are selected and enhanced with (1b-5b) HE method, (1c-5c) BBHE method, (1d-5d) DSIHE method, (1e-5e) BBCCE method and (1f-5f) PROICE method

synovial fluid and other neighbouring tissues. Thus, the designed framework could cause larger deviation from the enhancement result that it used to be. However, we claim that the value of standard deviation is acceptable from its coefficient of variation ($c_v = 0.053$, $c_v = \frac{std\ dev, \sigma}{mean, \mu}$), which is relatively small.

Besides, AMBE assesses the performance evaluation in terms of brightness preservation. Smaller AMBE indicates better brightness preservation and PROICE (0.020±0.007) ranks the first and followed by BBCCE (0.041±0.010) and BBHE (0.077±0.013). On the other hand, PROICE scores the highest SSIM value (0.935) among the methods which indicates that the structural similarity between original MR image and enhanced image is high and satisfying. Along three evaluation assessments, HE (SNR=9.471±0.386, AMBE=0.277±0.016, SSIM=0.430±0.037) is proven to be an unsuitable enhancement method for biomedical image as the dark gray levels occupy the majority gray levels of the MR image which could bring a sudden leap in CDF mapping curve.

However, there is trade-off between enhancement quality and time consumption for processing. PROICE spends longer time (0.425±0.215s) for a MR image compared to HE, BBHE, DSIHE and BBCCE (0.014±0.010s, 0.021±0.005s, 0.020±0.011s and 0.758±0.187s). Number of edges detected could determine the performance of enhancement methods, where the higher intensity of edges detected, the image is said to be well enhanced. However, ROI is the main enhancement priority and therefore the dark regions which consist of tibial and femoral bones will be washed out. The number of edges detection in PROICE (5600.600±367.724) is much lower than BBHE (6373.040±456.118), DSIHE (6557.090±422.112) and BBCCE (6293.510±338.673). With promising quality of image enhanced by proposed method, lower DE is still acceptable.

QUALITATIVE RESULTS

We take several criteria into consideration when evaluating PROICE enhanced image, which are tissue contrast enhancement, natural looking, brightness preservation and minimum image artifacts provocation. In Figure 3(1b – 5b), serious noise amplification can be observed in HE enhanced images as its mean brightness is not preserved in the algorithm. Annoying artifacts degrade the overall image's visual quality, and it causes difficulty in cartilage delineation. On the other hand, BBHE and DSIHE result better enhanced images than conventional HE method. However, it is challenging to distinguish the hyaline cartilage from its surrounding tissues and ligaments. Hence, BBHE and DSIHE are not suggested in enhancing biomedical images.

Thereafter, BBCCE was proposed to preserve the mean brightness while retaining the knee features. Typically, aforementioned contrast enhancement methods could lift the background luminance to a higher level due to steep CDF curve. BBCCE improves the overall brightness and the contrast of knee while avoiding background noise

amplification. Compared to BBCCE, PROICE is designed to improve the contrast difference between the knee cartilage and the surrounding tissues which makes the delineation process to be easier. The obvious gaps between articular cartilages and nearby cartilages or tissues are pointed with small red arrows which is as shown in Figure 3 (1f - 5f) the contrast of surrounding tissues is stretched to make the articular cartilages to be more visible and distinguishable. Notably, Marcelo claimed that intensity difference between degenerated region and normal healthy hyaline cartilage could be a way to detect chondral lesions (Rodrigues and Camanho 2010). Articular cartilage contains majority water, type II collagen and proteoglycans, hence it is brighter than other tissues in MR image. As cartilage surface starts to break down and degenerate, the intensity observed on MR image might be darker than its baseline image. Figure 3 (5f) shows that PROICE is highly sensitive to small intensity changes, thus it has great potential to detect cartilage thinning in the early progress.

CONCLUSION

Most contrast enhancement methods which use typical CDF curve are not suitable to be implemented into biomedical image processing. Traditional HE does not preserve its mean brightness and yet invariably shift the output mean brightness to its middle gray level. The resultant images are over-enhanced and some details of small regions will be washed out. PROICE is proposed to separate the input histogram into two sub-histograms while the breaking point is determined through GMM. On the other hand, Bezier transform curves are formed according to the sub-histograms. They are combined later, as a replacement of CDF curve, to equalize the original histogram. From the qualitative and statistical assessments, the proposed method is beneficial in terms of perceived visual quality, noise reduction and small error but it has trade-off of longer time in processing the image compared to other methods. To achieve a better enhancement result, denoise process is encouraged to be done prior to further contrast enhancement method. In a nutshell, PROICE is recommended to be carried out prior to knee cartilage segmentation stage for OA disease progression diagnosis as it offers great preservation of both ROI brightness and details.

DECLARATION OF COMPETING INTEREST

None.

ACKNOWLEDGEMENT

The authors would like to express their gratitude to Universiti Teknologi Malaysia and the Ministry of Higher Education (MOHE) Malaysia for supporting this research under Research University Grant (RUG), number R.J130000.7651.4C238. In addition, the authors would also

like to thank the Research Management Center (RMC) – UTM for supporting this research project.

REFERENCES

- Abdullah, W., Mohammad, Hasanul, K., Ali, A. D. & Oksam Chae. 2007. A dynamic histogram equalization for image contrast enhancement. *IEEE Transactions on Consumer Electronics* 53: 593-600.
- Asghar, Khurshid, Ghulam, G., Mubbashar, S. & Zulfiqar, H. 2017. Automatic enhancement of digital images using cubic Bézier curve and Fourier transformation. *Malaysian Journal of Computer Science* 30: 300-10.
- Barbour, Kamil, E., Charles, G. H., Michael B. & Teresa, J. B. 2017. Vital signs: prevalence of doctor-diagnosed arthritis and arthritis-attributable activity limitation—United States, *MMWR. Morbidity and mortality weekly report* 66: 246.
- Chen, Soong, D. & Abd, R. R. 2003a. Contrast enhancement using recursive mean-separate histogram equalization for scalable brightness preservation. *IEEE transactions on Consumer Electronics* 49: 1301-09.
- Chen, S.D. and Ramli, A.R. 2003b. Minimum mean brightness error bi-histogram equalization in contrast enhancement. *IEEE transactions on Consumer Electronics* 49(4): 1310-1319.
- Cheng, Fan, C. & Shih, C. H. 2013. Efficient histogram modification using bilateral Bezier curve for the contrast enhancement. *Journal of Display Technology* 9: 44-50.
- Cisternas, Miriam, G., Louise, M., Jeffrey, J. S., Daniel, H. S., David, J. P. & Charles, G. H. 2016. Alternative methods for defining osteoarthritis and the impact on estimating prevalence in a US population-based survey. *Arthritis Care & Research* 68: 574-80.
- Dar, S. U., Yurt, M., Karacan, L., Erdem, A., Erdem, E., & Çukur, T. 2019. Image synthesis in multi-contrast MRI with conditional generative adversarial networks. *IEEE Transactions on Medical Imaging* 38(10): 2375-2388.
- Dougherty, Geoff. 2009. *Digital Image Processing for Medical Applications*. Cambridge University Press.
- Gan, H. S., Tan, T. S., Abdul, K., Ahmad, H., Khairil, A. S., Abdul, K. R., Weng, K. T., Liang, X. W. & Kashif, T. C. 2014. Medical image visual appearance improvement using bi-histogram bezier curve contrast enhancement: data from the osteoarthritis initiative. *The Scientific World Journal*.
- Gan, H. S., Tan, T. S., Abdul, K. R., Abdul, K., Ahmad, H., Khairil, A. S., Liang, X. W. & Weng, K. T. 2014. Medical image contrast enhancement using spline concept: data from the osteoarthritis initiative. *Journal of Medical Imaging and Health Informatics* 4: 511-20.
- Huang, Shih, C. & Yeh, C. H. 2013. Image contrast enhancement for preserving mean brightness without losing image features. *Eng. Appl. Artif. Intell.* 26: 1487-92.
- Ismail, Wan, Z. W. & Kok, S. S. 2011. Contrast enhancement dynamic histogram equalization for medical image processing application, *International Journal of Imaging Systems and Technology* 21: 280-89.
- Kim, Y. T. 1997. Contrast enhancement using brightness preserving bi-histogram equalization. *IEEE transactions on Consumer Electronics* 43: 1-8.
- Kinoshita, Y. & Hitoshi, K. 2018. Automatic exposure compensation using an image segmentation method for single-image-based multi-exposure fusion. *APSIPA Transactions on Signal and Information Processing* 7.
- Mahajan, A. & Divya, G. 2017. Image contrast enhancement using Gaussian Mixture model and genetic algorithm. *International Conference On Smart Technologies For Smart Nation (SmartTechCon)* 979-83. IEEE.
- Mamoria, P. & Deepa, R. 2016. An analysis of images using fuzzy contrast enhancement techniques. *3rd International Conference on Computing for Sustainable Global Development (INDIACom)* 288-91. IEEE.
- Mukhopadhyay, S., Nirmalya, G., Ritwik, B., Prasanta, K. P., Sawon, P., Venkatesh, S. M. & Satyasan, C. 2015. An optimized hyper kurtosis based modified duo-histogram equalization (HKMDHE) method for contrast enhancement purpose of low contrast human brain CT scan images. *International Conference on Advances in Computing, Communications and Informatics (ICACCI)* 1819-21. IEEE.
- Narnaware, S. & Roshni, K. 2015. Image enhancement using artificial neural network and fuzzy logic." *International Conference on Innovations in Information, Embedded and Communication Systems (ICIIECS)* 1-5. IEEE.
- Nnolim, U. A. 2018. Partial differential equation-based hazy image contrast enhancement. *Computers & Electrical Engineering* 72: 670-681.
- Pathak, Sampada, S., Prashant, D. & Ganesh, P. 2015. A combined effect of local and global method for contrast image enhancement. *IEEE International Conference on Engineering and Technology (ICETECH)* 1-5. IEEE.
- Pizer, Stephen, M., Eugene, J. R., James, P. E., Bonnie, C. Y. & Keith, E. M. 1990. Contrast-limited adaptive histogram equalization: speed and effectiveness. *Proceedings of the First Conference on Visualization in Biomedical Computing* 337-45. IEEE.
- Rodrigues, Marcelo, B. & Gilberto, L. C. 2010. Mri evaluation of knee cartilage, *Revista Brasileira de Ortopedia (English Edition)* 45: 340-46.
- Rundo, L., Andrea, T., Marco, S. N., Carmelo, M., Daniela, B., Giancarlo, M. & Paolo, C. 2019. MedGA: A novel evolutionary method for image enhancement in medical imaging systems. *Expert Systems with Applications* 119: 387-99.
- Singh, H., Kumar, A., Balyan, L. K. & Singh, G. K. 2018. Swarm intelligence optimized piecewise gamma corrected histogram equalization for dark image enhancement. *Computers & Electrical Engineering* 70: 462-475.
- Styner, M., Christian, B., Szckely, G. & Guido, G. 2000. Parametric estimate of intensity inhomogeneities applied to MRI. *IEEE Trans. Med. Imaging* 19: 153-65.
- Teh, V., Kok, S. S. & Eng, K. W. 2018. Contrast enhancement of CT brain images using gamma correction adaptive extreme-level eliminating with weighting distribution. *International Journal of Innovative Computing, Information and Control* 14: 1029-41.
- Thakur, A. & Deepak, M. 2015. Fuzzy contrast mapping for image enhancement. *2nd International Conference on Signal Processing and Integrated Networks (SPIN)* 549-52. IEEE.

- Tian, Q. C. & Laurent, D. C. 2018. A variational-based fusion model for non-uniform illumination image enhancement via contrast optimization and color correction. *Signal Processing* 153: 210-20.
- Wang, Y. F., Qian, H. & Jing, H. 2018. Adaptive Enhancement for Low-Contrast Color Images via Histogram Modification and Saturation Adjustment. *IEEE 3rd International Conference on Image, Vision and Computing (ICIVC)* 405-09. IEEE.
- Wang, Y., Qian, C. & Baoomin, Z. 1999. Image enhancement based on equal area dualistic sub-image histogram equalization method. *IEEE transactions on Consumer Electronics* 45: 68-75.
- Wongsritong, K., Kittayaruasiriwat, K., Cheevasuvit, F., Dejhan, K. & Somboonkaew, A. 1998. Contrast enhancement using multipeak histogram equalization with brightness preserving. *IEEE Asia-Pacific Conference on Circuits and Systems. Microelectronics and Integrating Systems. Proceedings (Cat. No. 98EX242)* 455-58. IEEE.
- Yang, K. F., Hui, L., Kuang, H. L., Chao, Y. L. & Li, Y. J. 2018. An Adaptive Method for Image Dynamic Range Adjustment. *IEEE Transactions on Circuits and systems for video technology* 29: 640-52.
- Yelmanova, E. S. & Yuriy, M. R. 2017. Adaptive enhancement of monochrome images with low-contrast objects. *12th International Scientific and Technical Conference on Computer Sciences and Information Technologies (CSIT)* 421-24. IEEE.
- Zarie, M., Hassan, H. & Abdollah, E. M. 2018. Contrast enhancement using triple dynamic clipped histogram equalization based on mean or median. *Optik* 175: 126-37.